


Article

MCNP and CFD Modeling for Potential High-Power Configuration of Missouri S&T Reactor

Thaqal M. Alhuzaymi ^{1,2}, Meshari M. ALQahtani ^{1,2}, Thaar M. Aljuwaya ^{1,2,*}  and Ayodeji B. Alajo ¹

¹ Nuclear Engineering and Radiation Science Department, Missouri University of Science and Technology (Missouri S&T), Rolla, MO 65409, USA

² Nuclear Technologies Institute, King Abdulaziz City for Science and Technology (KACST), P.O. Box 6086, Riyadh 11442, Saudi Arabia

* Correspondence: taljuwaya@kacst.edu.sa; Tel.: +966-11-481-4016

Abstract: Utilization of nuclear research reactors is of high importance for education and training, research and development, and many other applications. However, less effective utilization encountered in research reactors is mainly due to limitations in power levels and related experimental facilities. Such limitations, however, have led different global owners of research reactors to consider upgrading the power levels of their reactors to accommodate the increase in utilization demands. To consider upgrading the power levels of research reactors without replacing major components, a pair of essential analyses must be performed, namely the neutronic evaluation of nuclear fission and thermal-hydraulic evaluation for heat removal from the reactor core. In this work, a conceptual upgrade to the core design and configuration of MSTR, or Missouri University of Science and Technology Reactor (200 kilowatts (kW)), is demonstrated. The conceptual design of the MSTR high-power configuration (MSTR-HPC) aims to achieve high neutron flux and demonstrate the power level and core configuration with greater flexibility and adaptability while not exceeding safety limits. The conceptual design of the MSTR-HPC involves upgrading the power level to 2 megawatts (MW), reconfiguring the core, changing the fuel meat type, inclusion of a flux trap (FT) facility, and others. In addition, the conceptual design of MSTR-HPC includes three in-core irradiation facilities, namely FT, bare rabbit tube (BRT), and cadmium rabbit tube (CRT). The neutronic evaluation of the MSTR-HPC was carried out using the Monte Carlo N-particle Code (MCNP), version 6. In addition, the thermal-hydraulic behavior of MSTR-HPCs' hot-channel has been assessed by means of ANSYS Fluent to evaluate the satisfaction of thermal-hydraulic safety requirements of the conceptual design. The results obtained have shown that the conceptual MSTR-HPC has demonstrated a maximum neutron flux obtained higher than that obtained in the current MSTR core by two orders of magnitude. The conceptual design of MSTR-HPC with composite BeO/graphite reflector blocks was able to sustain critically and operate continuously at full power for 61 days. In regards to the hottest fuel plate of MSTR-HPC, the results have shown that the determined temperature for the fuel plate regions was below the safety limits. In addition, at full operation power of the MSTR-HPC, the mass flow rate of 39.86 kg/s (10.644 gallon/s) was sufficient for removing the generated heat. In conclusion, the conceptual design of the MSTR-HPC has demonstrated its flux enhancement capabilities while maintaining safety limits, which are of high importance in enhancing reactor utilization for a larger window of time.



Citation: Alhuzaymi, T.M.; ALQahtani, M.M.; Aljuwaya, T.M.; Alajo, A.B. MCNP and CFD Modeling for Potential High-Power Configuration of Missouri S&T Reactor. *Processes* **2023**, *11*, 1044. <https://doi.org/10.3390/pr11041044>

Received: 20 February 2023

Revised: 26 March 2023

Accepted: 28 March 2023

Published: 30 March 2023



Copyright: © 2023 by the authors. Licensee MDPI, Basel, Switzerland. This article is an open access article distributed under the terms and conditions of the Creative Commons Attribution (CC BY) license (<https://creativecommons.org/licenses/by/4.0/>).

Keywords: reactor design; high power configuration; neutron flux spectrum; MCNP; CFD

1. Introduction

The nuclear industry, along with many other fields, owes its continued advancements in research, development, and overall improvement to research reactors [1–3]. Research reactors can be used for many purposes, including isotope production, materials testing, education, and training [1,2,4]. The primary goal of a research reactor in any case, however,

is the production of useful neutrons, i.e., in medicine, manufacturing, agriculture, etc. Low- and intermediate-energy neutrons (i.e., thermal or epithermal neutrons, respectively), which are produced by thermal research reactors, can be used for a breadth of important purposes [1,2]. Among these purposes are neutron radiography, NAA (Neutron Activation Analysis), low-scale isotope production, basic irradiation experiments, and much more. In the investigation of fast neutron damage or high-energy neutron dose, however, hard spectra are required. With the appropriate mixture of energy and flux, advanced materials testing and large-scale isotope production can greatly benefit. A challenge to the effective use of research reactors is the problem of sustaining fast neutrons in highly moderated surroundings [1,5]. To solve such an issue, some research reactors have design parameters that allow them to operate specifically in the fast spectrum. There are several such reactors, including FFTF (Fast Flux Test Facility), HFIR (High Flux Isotope Reactor), and ATR (Advanced Test Reactor) [5–8]. Nonetheless, there are still issues with these research reactors when research requires thermal neutrons. Due to the high frequency of experimentation with thermal neutrons, thermal and hard spectra are often needed. Hence, there is considerable demand for a single reactor with a flexible core configuration that can combine both types of spectra and allow for diverse irradiation experiments with one apparatus. The aforementioned perspective is the prime motivation for this work.

This work demonstrates a conceptual upgrade of the Missouri University of Science and Technology Reactor (MSTR) power. The objective is to explore the possibility of avoiding the rigidity associated with MSTR's traditional design, introducing the flexibility and adaptability necessary to support a broader range of utilization and experimental research. A conceptual upgrade to MSTR core design and configuration is therefore proposed, involving neutronic evaluation. This conceptual upgrade has the following objectives: (1) in-core irradiation with high neutron flux and (2) adaptable/flexible power level and core configuration. This will allow the core to be configured for both a low-power and high-power mode. The reactor core components can be shuffled around in the core, and the reactor's power level can be adjusted accordingly, allowing for a shift in power output. This study focuses on the proposed high-power mode of such a concept. With that perspective mentioned, it is also essential to take into high consideration, along with the conceptual upgrade, thermal-hydraulic behavior. Requirements for cooling and heat removal, for instance, are crucial to the safety of the new design. Heat is primarily released in the structural materials of fuel plates and transferred from fuel to the adjacent coolant "water" channel. The heat must be removed and transferred properly to prevent the structural materials' temperature from expanding above safety limits which trigger fuel melting and release of radionuclides. The maximum heat over the entire core is generated in the hottest fuel plate. Under the anticipated normal operation conditions, the reactor can be considered to operate safely if the generated heat in the hottest fuel plates can be safely transferred through the structural materials and safely removed by the coolant channel. With this perspective in mind, this study also evaluates the thermal-hydraulic safety requirements of the hot channel of the MSTR-HPC using ANSYS Fluent. In particular, the thermal-hydraulic properties of the hot channel of MSTR-HPCs are examined from the point of view of safety limits.

The MSTR is a research reactor of the open pool type built-in 1961. While it has experimental and research applications, it is also used for training and education in nuclear engineering [9–11]. Research utilization of the MSTR includes neutron radiography, NAA, image processing, radiolysis, and more, with an operational power level of up to 200 kilowatts (kW) [10]. Moderation and natural convective heat removal are carried out using light water, and MSTR plate-type fuel is used in the fuel element. MSTR's grid plate can take 54 positions comprising a nine-by-six aluminum array. There are nineteen fuel elements, three in-core irradiation facilities, and one source holder within the MSTR core (see Figure 1 for the MSTR current core configuration). The control rods comprise four fuel elements to control reactor power. These positions are indicated in Figure 1 at C5, D7, E5, and E7. MSTR houses a primary and secondary coolant system, where the primary is

made up of a reactor pool, the pool water makeup system, a Nitrogen-16 control system, and a demineralizer. The secondary system consists of a heat exchanger, chiller, processed water with chilled loops, and a control unit. The secondary coolant system was installed in 2013 to allow for active heat removal, improving heat removal rates and preventing heat buildup in the reactor pool. Further details about the MSTR-related systems can be found elsewhere [10–15].

	1	2	3	4	5	6	7	8	9
A									
B						S			
C					CR4	FE	FE	FE	
D				FE	FE	FE	CR1	FE	FE
E				FE	CR3	FE	CR2	FE	FE
F				CRT	FE	HC	FE	BRT	FE

Figure 1. MSTR current core configuration called the “120 W” configuration. S: Source Holder; FE: Fuel Element; CR#: Control Rod; HC: Hot Cell; BRT: Bare Rabbit Tube; CRT: Cadmium Rab-bit Tube.

The MSTR flux spectrum and hot channel in a variety of configurations have been experimentally determined on many occasions. The MSTR flux spectrum has been characterized experimentally by means of an activation-foil method [10]. The foils were irradiated at location B6 at 100 kW in the current MSTR core configuration, as outlined in Figure 1 (“120 W”). SAND-II and Monte Carlo N-Particle (MCNP) codes with unfolding method implementations were used to determine the neutron spectra, which were $4.79 \times 10^{11} \pm 6.10 \times 10^{10}$ and $4.98 \times 10^{11} \pm 1.72 \times 10^{10} \text{ n cm}^{-2} \text{ s}^{-1}$ respectively [10]. In 2010, Zachary Kulage characterized the 120 W MSTR configuration by carrying out a similar foil activation analysis with SAND-II and MCNP codes at full power, or 200 kW [13]. At full power, the thermal, intermediate, and fast neutron flux was determined to be $2.94 \times 10^{12} \pm 1.9 \times 10^{10}$, $1.86 \times 10^{12} \pm 3.7 \times 10^{10}$, and $2.65 \times 10^{12} \pm 3.0 \times 10^3 \text{ n cm}^{-2} \text{ s}^{-1}$, respectively, with a total flux of $7.55 \times 10^{12} \pm 5.7 \times 10^{10} \text{ n cm}^{-2} \text{ s}^{-1}$ [13]. The maximum total flux achievable according to an MSTR safety analysis is $4.36 \times 10^{12} \pm 2.84 \times 10^{11} \text{ n cm}^{-2} \text{ s}^{-1}$ [11,14]. O’Bryant et al. [15] found both the clean core (no poison buildup and zero burnups) and burned core hot-channel for the MSTR 120 kW configuration using MCNP code via tracking of fission energy deposition. It was found to be located between fuel plates six and seven of CR1 for both, with no shift in either core (CR1 is located at D7—see Figure 1) [15]. The power peaking factors were reported to be 1.85 and 1.71, respectively, for the clean and the burned cores [15].

2. The Proposed MSTR High-Power Configuration (MSTR-HPC)

The MSTR high-power configuration (MSTR-HPC), or high-power mode, that we propose aims to achieve high neutron flux to enable advanced research and experimentation. Based on the current MSTR configuration, MSTR-HPC will be designed with features modified to achieve high neutron flux. The following features are to be modified: (1) power level updated; (2) fuel meat type and fuel meat design; (3) addition of flux trap facility; (4) reactor core reconfiguration; and (5) control rod boron concentration increase to ensure

effective shutdown. The evaluation of such modifications, the conceptual upgrade design of the MSTR, is carried out via the MCNP simulation, where the simulation is designed to update the MSTR power level power from 200 kW up to 2 MW. Since the neutron flux magnitude is directly proportional to reactor power, an increase in the power level will yield a corresponding increase in the neutron flux [16]. For the MSTR, the low density of current MSTR fuel (5.5 g/cm^3) with low enrichment levels (19.75% ^{235}U enriched) makes it impossible to use such fuel for a high-power configuration [10,14]. The MSTR fuel is not able to provide adequate reactivity, neutron flux, burnup, and many other important features [17]. Perhaps more crucially, core criticality would also be difficult to maintain with respect to the core configuration [17]. Different US research reactors of High-power (e.g., the Missouri University Research Reactor (MURR), the Massachusetts Institute of Technology Reactor (MITR)) use UAl_x fuel instead. The UAl_x fuel has a low density ($\sim 3.6 \text{ g/cm}^3$) but is very highly enriched (93% ^{235}U enriched), allowing it to overcome the alloy's low physical density and provide the necessary performance [16,17]. To convert fuel to LEU, uranium-10 wt% molybdenum metallic alloy (U-10Mo) with 19.75% enriched ^{235}U was chosen as the best candidate by the US Department of Energy's (DOE) reduced enrichment for research and test reactor (RERTR) program [12,16–20]. This was due to the very high uranium density of U-10Mo (16.09 g/cm^3), along with its stability and predictable irradiation behavior program. An undesirable reaction occurs, however, between U-10Mo foil and aluminum, and a diffusion barrier is therefore required to avoid blistering and delamination program [12,16–20]. In cases of high burnup or high fission rate, U-10Mo foil, and aluminum could interact to cause swelling [16]. U-10Mo fuel has exhibited blistering and delamination in high-temperature experimental environments [21]. The proposal from RERTR is to surround the fuel meat with a thin layer of zirconium ($25.4 \mu\text{m}$) as a diffusion barrier program [12,16–20]. However, there are still problems with U-10Mo due to its aluminum cladding's inability to accommodate fission gas buildup in a plate-type fuel. As of this writing, U-10Mo fuel is still under development and qualification. To this end, MITR, and MURR have each performed thermohydraulic and neutronic studies while considering U-10Mo fuel. U-10Mo is therefore the best candidate fuel available for MSTR-HPC. As suggested, the MSTR fuel plate is modified to include a thin zirconium layer (see Figure 2).

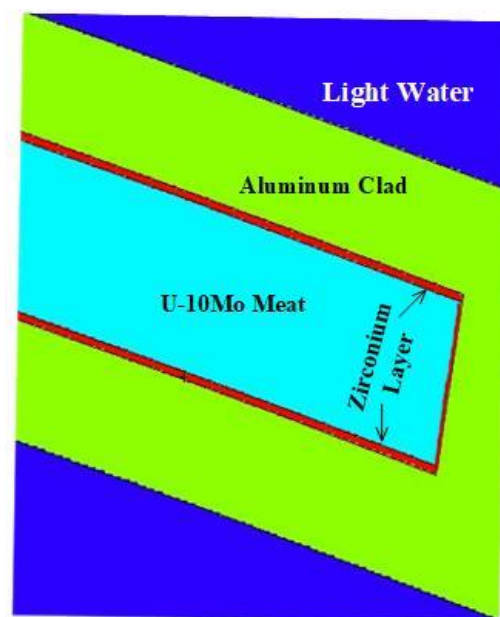


Figure 2. Middle-Cut-View of a single fuel plate containing U-10Mo meat surrounded by a thin zirconium layer, aluminum clad, and light water.

To further advance the MSTR-HPC utilization, a flux trap (FT) facility is included in addition to the above modifications. This FT facility is situated in the reactor core, near

the center. With the FT, neutron flux will be concentrated in a specific region (central reactor core) where the neutron population is highest. The flux trap is cylindrical, 3.2 cm in diameter and 60 cm in height, and is located inside the hollowed-out shell of a standard fuel element. CRT and BRT were also considered as irradiation facilities for MSTR-HPC, for which the design geometry would remain unchanged, as it exists at present in the MSTR core. A compact core concept is adopted for the MSTR-HPC reactor core reconfiguration, as shown in Figure 3. The current grid plate is replaced with a 9×9 aluminum array (see Figure 1 for the current design), allowing 81 positions. This new core arrangement comprises four control rods, four fuel elements, and three irradiation facilities: FT, BRT, and CRT (see Figure 3). Graphite blocks surround the compact core, providing neutron reflection and helping to maintain the core at criticality. These blocks are graphite-filled standard fuel element shells. Graphite is chosen for its affordability and well-known reflective properties, though Beryllium Oxide (BeO) is also considered a reflector. BeO is more expensive than graphite, but a better neutron reflector, owing to its thermal absorption and scattering cross-sections [22,23]. Nonetheless, graphite was chosen as the primary reflector for MSTR-HPC, and a thin slab (0.5 cm) of BeO was introduced to the reflector blocks and studied for neutronic effects in the current work. The central grid (D4:F6), 3×3 , contains the fuels, as illustrated in Figure 3. Finally, MSTR-HPC has a fifth modified feature, which is its increased boron concentration in control rods. The concentration of boron was raised to 2% to allow for effective safety shutdown.

	1	2	3	4	5	6	7	8	9
A									
B						GB			
C			GB	GB	GB	BRT	GB		
D			GB	FE	CR1	FE	GB		
E			GB	CR4	FT	CR3	GB		
F			GB	FE	CR2	FE	GB		
G			GB	GB	GB	CRT	GB		
H						GB			
L									

Figure 3. The proposed MSTR high-power core configuration. GB: Graphite Block; FE: Fuel Element; CR#: Control Rod; BRT: Bare Rabbit Tube; CRT: Cadmium Rabbit Tube; FT: Flux Trap.

In order to evaluate the neutronic properties of the MSTR-HPC, the Monte Carlo N-particle Code (MCNP), version 6, will be used. MCNP is an advanced, versatile, well-validated code to simulate neutronic phenomena. It can accurately calculate neutron flux distributions, radiation dose rates, and other parameters. MCNP is suitable for the MSTR-HPC evaluation, as it is capable of handling compact geometries. MCNP is used first to analyze the criticality of the MSTR-HPC. After ensuring criticality, the shutdown margins are evaluated by analyzing the value of two shutdown control rods using MCNP. This helps to ensure that the reactor can be safely shut down if necessary. The control rods absorb

neutrons, which can be used to slow down the reaction and reduce the power in the reactor. After that, the neutron flux amp and capabilities of the MSTR-HPC are assessed via MCNP. The maximum neutron flux is determined by evaluating the neutron flux distribution. Thus, it is possible to determine whether or not the hard flux obtained was in the proposed flux trap. This allows for the optimization of the neutron flux trap design to ensure that the maximum neutron flux is achieved without exceeding safety limits. Then, a burnup analysis is performed to determine how long the reactor will operate. Burnup analysis is important in order to determine how long the reactor will be able to safely produce energy before it needs to be shut down or refueled. The next step is to verify that the heat generated in the core can be removed safely. This can be achieved by first determining from the MCNP's results of energy deposition across the MSTR-HPC core which channel is the most heated. After the energy deposition is evaluated, a thermal analysis is conducted to determine the steady-state temperature distribution across the core in order to ensure that the hot channel is cooled sufficiently. This is accomplished by simulating the coolant's flow and heat transfer performance in the hot channel using ANSYS Fluent software. The results are then compared to the allowable temperature limits of the core to determine if the heat generated in the core can be safely removed.

3. MCNP Model and Simulation Conditions

To represent the MSTR-HPC proposal, modifications were made to a high-fidelity MCNP model of the MSTR facility that already exists. U-10Mo fuel with a thin zirconium layer was added as a modification to the fuel plate models in his high-fidelity version, leaving the curved fuel plate's total thickness unaltered (0.13 cm). The original thickness of the cladding was 0.0395 cm, and the thickness of the zirconium was subtracted from this to ensure the total final thickness was the same, leaving the new cladding thickness on either side of the fuel meat at 0.0392 cm. Both the current MSTR and the proposed MSTR-HPC have their fuel plate dimensions presented and compared in Table 1. Remaining modifications included: (1) grid plate change to 9×9 aluminum array; (2) four fuel elements repositioned; (3) four control rods (three shim safety rods and one regulating rod) repositioned; (4) Flux trap (FT) facility included as previously described; (5) CRT and BRT repositioned; and (6) block reflectors surrounding the core added.

Table 1. Dimensions comparison of fuel plate for current MSTR and MSTR-HPC.

	Current MSTR	MSTR-HPC
Width of Fuel Meat	0.051 cm	0.051 cm
Length of Fuel Meat	61 cm	61 cm
Thickness of Clad	0.0395 cm	0.039246 cm
Thickness of Zirconium	-	0.000254 cm
Total Thickness of Fuel Plate	0.13 cm	0.13 cm
Water Gap Between Plates	0.31 cm	0.31 cm

To carry out the simulation of MSTR-HPC with all necessary modifications, the requirements were as follows:

1. The neutron multiplication factor (k_{eff}) needs to be determined.
2. The optimal graphite-to-BeO thickness ratio needs to be analyzed.
3. CR safety shutdown margin needs to be determined.
4. Determination of neutron flux map over MSTR-HPC core and neutron flux spectrum in-core irradiation facilities.
5. Burnup analysis.
6. Hot-channel needs to be identified for clean core and burned core.

To determine "excess reactivity," or k_{eff} , a KCODE criticality calculation was set up with all control rods completely withdrawn using 20,000 particles per cycle, 300 active cycles, and 20 discarded cycles. KCODE is a term used in the MCNP cards for determining

the specifications of the criticality source. The actual geometry of the core had a mesh card set up around it to allow for full power (2 MW) flux map analysis. Tally F4:N was used to determine the flux spectrum in the in-core irradiation facilities at full power. ENDF/B-VI was used as a cross-sectional data library for all model isotopes. The cross-section was modified to the desired operating temperature using a temperature card, ranging from 300 K to 350 K, depending on need. A burnup card from the MCNP model was used for burnup analysis, demonstrating the length of time for which criticality could be sustained in the reactor core. Full-power hot-channel determination was determined using a single mesh for each core fuel plate (a total of 112) to track fission energy deposition. Fission energy deposition was tracked using tally F7:N at each fuel plate. MCNP version 6 was used for all simulations [24].

4. Modeling specifications of the MSTR-HPCs' Hot-Channel

As mentioned previously, the thermal-hydraulic of MSTR-HPCs' hot-channel from a safety limits perspective has to be assessed. Therefore, ANSYS software [25] was used to model heat generated in the fuel plate, making sure this not exceeding safety limits. The model contains two parallel curved half-fuel plates encountered in MSTR, along with a single coolant channel between the two plates. Figure 4 shows the cross-sectional view of the represented model. Different geometrical parameters for the curved fuel plates of the MSTR-HPC as well as the coolant channel were taken into account. The model was designed and set up using ANSYS software 17.2. Regarding the computational domain, it was 62.5 cm tall, 1.25 cm wide, and 6.68 cm in length. For the coolant channel, the determined Reynolds number was 3799. The simulation has been carried out, presuming a steady-state single-phase turbulent flow. In addition, forced circulation was assumed for removing heat with an inlet temperature of 322.15 K for the coolant channel. For conservative analyses, the 32.42 kW, which is the full power generated, was separated among both curved fuel plates of the MSTR-HPC. This means that each one of the fuel plates produced total power equal to 16.21 kW. The heat generation has been considered uniform volumetric heat for every single fuel region. The defined total volumetric heat rate was about 1744.5 W/cm^3 .

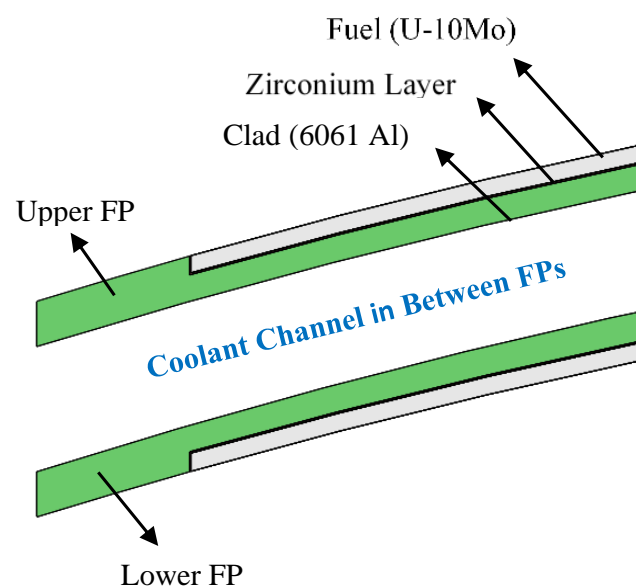


Figure 4. Cross-sectional-view of the simulated MSTR-HPCs' hot-channel.

Thermal hydraulic parameters for the model are presented in Table 2. Based on the design, ΔT was 12 K, and the total coolant cross-sectional area for the active core was calculated to be 332.5 cm^2 . The calculated total mass flow rate was 39.86 kg/s . For the coolant channel, the calculated cross-sectional area and mass flow rate were 2.071 cm^2

and 0.248 kg/s, respectively. The determined inlet velocity for the core was 1.213 m/s. Considering the 26 ft (7.9248 m) deep-water as of the MSTR reactor pool, the calculated outlet pressure was 178.78 KPa. The surface walls bounded the coolant channel, and the two fuel plates were assumed to be adiabatic, as shown in Figure 5. The no-slip condition was applied for the interface of the coolant channel with the convex and concave sides of the fuel plates. This implies zero velocity at the interfacing surfaces (clad with coolant), which will result in high temperatures than in a real-life situation. Thus, for conservative analysis, the no-slip condition was applied. No nucleate boiling is allowed throughout the simulated model. The model boundary conditions and solving algorithm are presented in Table 3. The inlet and outlet conditions of the computational domain were set to be mass flow rate and pressure, respectively. Standard (SST) κ - ω was chosen for solving Reynolds-averaged Navier-Stokes equations. The governing equation for the conservation of mass, momentum, and energy was solved by FLUENT.

Table 2. Thermal hydraulic parameters.

Fuel	U-10Mo
Fuel Thermal Conductivity (W/cm k)	0.176
Fuel Density (g/cm ³)	16.09
Coolant	Light Water
Coolant Flow Direction	Upward
Water Specific Heat (J/kg k)	4181.5
Cladding	Al 6061
Cladding Thermal Conductivity (W/cm k)	1.67
Cladding Density (g/cm ³)	2.7
Zirconium Density (g/cm ³)	6.506
Zirconium Thermal Conductivity (W/cm k)	0.23
Inlet Temperature (k)	322.15
Outlet Pressure (Pascal)	178,788.12
Mass Flow Rate (kg/s) for Coolant	0.24823
Cross-Sectional Area for Coolant (cm ²)	2.0708
Total Power Distribution by Fuel Plates (W)	32,416.06
Total Volumetric Heat Rate (W/cm ³)	1744.5
Reynolds number for Coolant	3799.88
Prandtl number	4.39

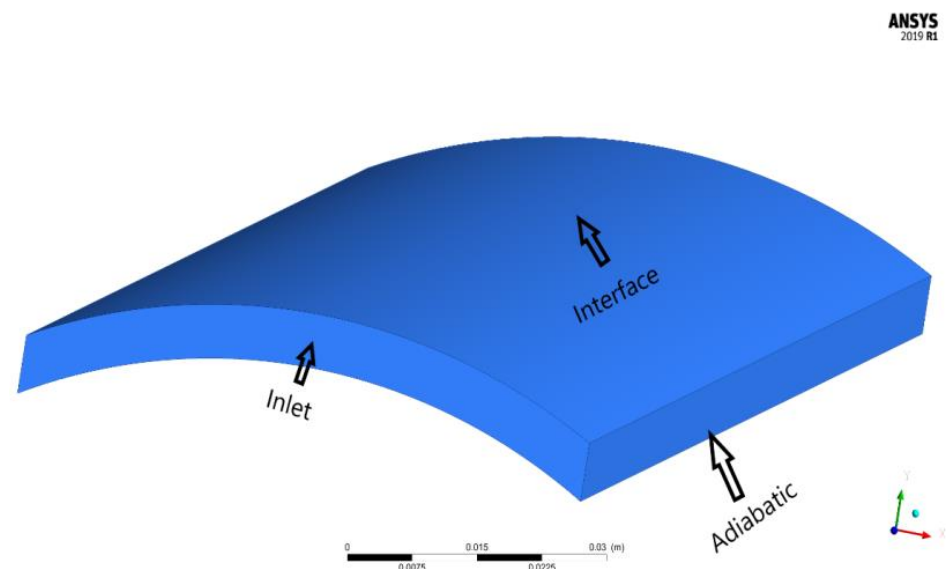
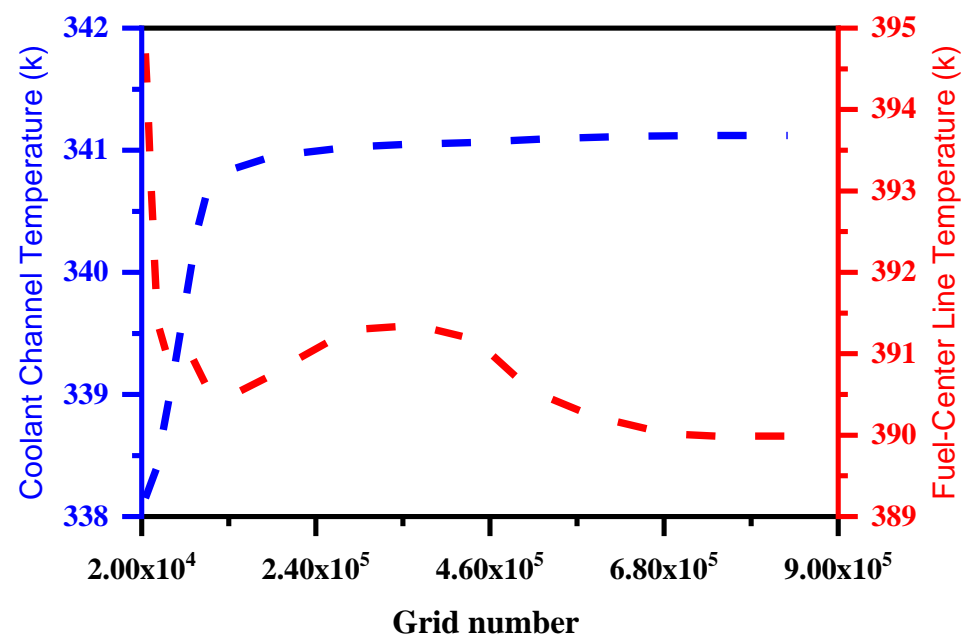


Figure 5. Boundary conditions of coolant channel.

Table 3. Boundary conditions, solving algorithm, and mesh parameters.

Turbulence Model	Standard (SST) κ - ω
Inlet Condition	Mass flow rate
Outlet Condition	Pressure Outlet
Wall Between Fuel and Cladding	Coupled
Wall Between Cladding and Coolant	Fluid Solid Interface
Parameters	Number
Node of Single Fuel Region	78,208
Node of Single Clad Region	89,130
Total Node of Solid	334,676
Total Node of Fluid	345,261

Element sizing function was applied to mesh the fuel plates. Due to the limitation of computational resources, the smallest element size that can be successfully generated is 1 mm. The edge sizing function was applied along the height, length, and width of the coolant channel. Several grid numbers were considered for evaluating mesh sensitivity, see Figure 6. The considered total nodes were 24,689, 35,497, 40,749, 65,488, 91,216, 107,397, 268,362, 351,251, 451,005, 679,937, 758,315 and 836,693. From the smallest considered grid number to the maximum, the temperature variation for the coolant channel and fuel center line were 2.97 and 4.70 K, respectively. Thus, the temperature of the coolant channel at the outlet and fuel center line was not significantly changed. Grid number with total nodes of 679,937 (see Table 3) was considered for performing the CFD simulation. Such selection help minimize the computational requirements.

**Figure 6.** Evaluation of mesh sensitivity of the simulated MSTR-HPCs' hot-channel.

For better evaluation of heat transfer over a small region, the thin zirconium layer surrounding the fuel meat was defined as thermal contact conductance (TCC) [25]. TCC was determined by dividing the thermal conductivity of zirconium by its thickness; $TCC = 90.55 \text{ W/cm}^2\cdot\text{K}$. Three locations were assigned for data extraction of the simulated coolant model, namely, inlet, middle, and outlet.

5. Results and Discussion

5.1. Determination of k_{eff} and Safety Shutdown Margin

To determine the reactivity coefficient (k_{eff}), the reflector blocks were filled entirely with graphite, and the control rods were fully withdrawn. The measurement was made at room temperature, with k_{eff} determined at 1.02239 and a standard deviation of 0.00036. To determine the safety shutdown margin, the shutdown control rods are assumed (two pairs of CRs), wherein the second pair, one control rod is an extra shutdown control rod, and the other is the regulating control rod. All four control rod positions are used to test both pairs: D5-(CR1), E4-(CR4), E6-(CR3), and F5-(CR2), as seen in Figure 3. CR1 and CR2 are found to be the positions of the effective shutdown CRs, with k_{eff} equal to 0.93395 with an estimated standard deviation of 0.00037 when CR1 and CR2 are fully inserted. Figure 7 shows a plot of the worth of these control rods. The regulating control rod and extra shutdown control rod were assigned to CR3 and CR4, respectively.

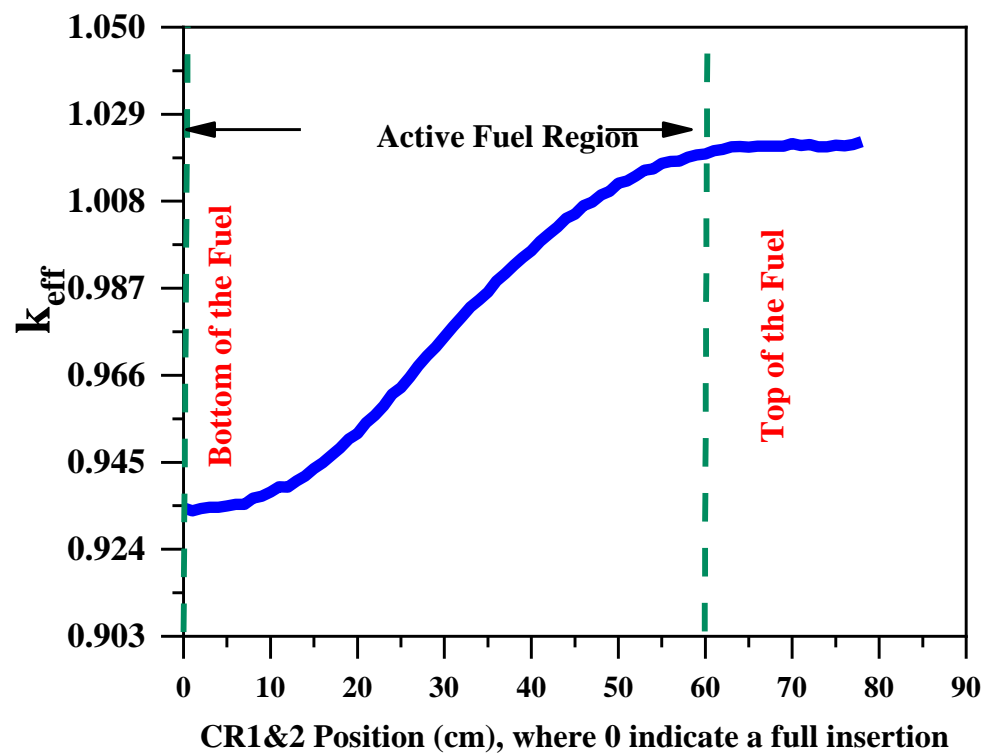


Figure 7. The worth of pair shutdown control rods (CR1 and 2).

5.2. Analyzing the Optimum BeO to Graphite Thickness Ratio

The neutronic performance is improved by using the optimal BeO to graphite thickness, allowing for MSTR-HPC core operation cycles to be longer. The MSTR-HPC core was originally surrounded by reflector blocks filled with graphite only. By measuring its effects on peak-to-average flux ratio and k_{eff} , an optimal BeO to graphite ratio was found, and the MCNP simulation was carried out iteratively. First, reflector blocks with 100% graphite were used, with iterative 0.5 cm BeO slabs added, keeping the total reflector thickness constant. The reflector slabs were oriented vertically with variation in thickness orthogonal to the vertical axis of the core, with the BeO side of the reflectors bounding the core in all cases where BeO/graphite reflectors were simulated. Figure 8 shows the k_{eff} and peak-to-average flux ratio for varying BeO/graphite composites, where the x -axis represents block thickness in centimeters, starting from 0.00 cm (side adjacent to the core center) and running to 7.6 cm (block outer region); the left y -axis represents k_{eff} (blue line); and the right y -axis represents the peak-to-average flux ratio (red line).

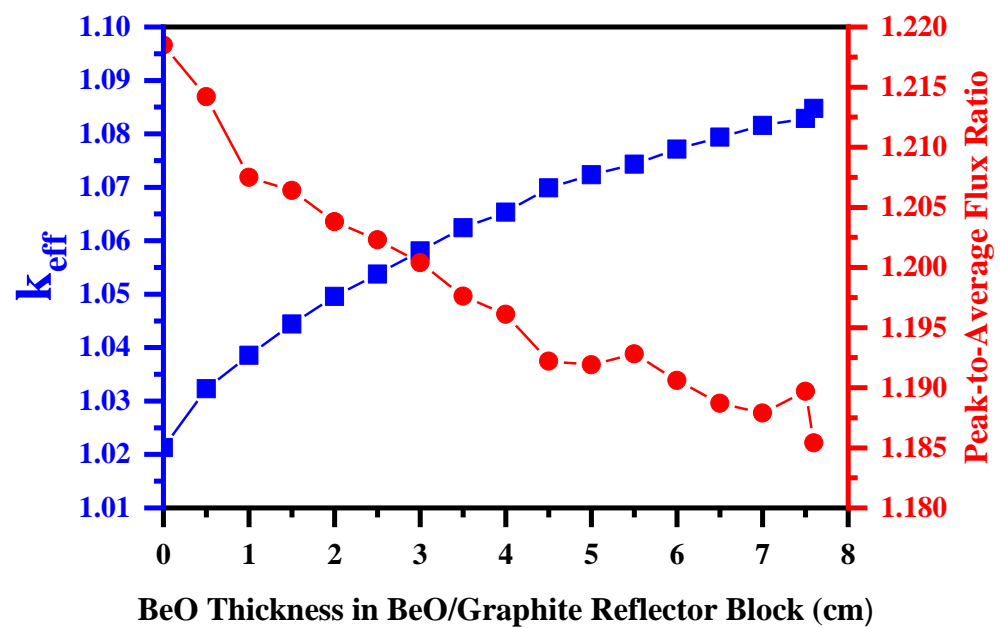


Figure 8. Impact of BeO/Graphite composite reflector block on multiplication factor and peak-to-average flux ratio. 0 cm implies 100% graphite block, while 7.6 cm implies 100% BeO block.

With a full graphite block, i.e., BeO thickness equaling 0.00 cm, k_{eff} was determined to be 1.0223, and the peak-to-average flux ratio was 1.2185. At 0.5 cm BeO, k_{eff} increased, and the peak-to-average flux ratio decreased. A block composed fully of BeO saw a significant increase in k_{eff} to 1.08747 and a decrease in the peak-to-average flux ratio to 1.1854. Minimizing the thickness of BeO in the reflector block composite is ideal due to the high expense associated with beryllium. The current limitations on excess reactivity with MSTR are 1.5% $\Delta k/k$ [26]. However, the uprated power level of MSTR-HPC allows the authors to assume an excess reactivity limit three times higher, implying a maximal k_{eff} of 1.04712. This limit was satisfied by a BeO thickness of 1.5 cm, as shown in Figure 8. Characterizing the flux profile flatness is the peak-to-average flux ratio, which was found to be identical at either 1 cm or 1.5 cm BeO thickness. A 1 cm thickness was therefore chosen for the reflector composition in this proposed model. This thickness yielded a k_{eff} of 1.03853 and a peak-to-average flux ratio of 1.2075, again shown in Figure 8.

5.3. Neutron Flux Map and Capabilities

Figure 9 provides an overview of the MSTR-HPC core neutron flux profile. The neutron flux is highest in the reactor core's central region (shown in the darkest red color). This is the flux trap region. Here, the MCNP-calculated total neutron flux is $1.42 \times 10^{14} \pm 1.78 \times 10^{12} \text{ n cm}^{-2} \text{ s}^{-1}$. Respectively, the MCNP-calculated total neutron flux for the BRT and CRT were $8.23 \times 10^{13} \pm 6.48 \times 10^{12} \text{ n cm}^{-2} \text{ s}^{-1}$ and $4.15 \times 10^{13} \pm 4.63 \times 10^{12} \text{ n cm}^{-2} \text{ s}^{-1}$.

The neutron flux spectra from MSTR-HPC in-core irradiation facilities are presented in Table 4 and Figure 10. The fast flux contributes the most at the FT facility, providing 35.52% of the total produced flux, with 32.28% and 32.21%, respectively, for resonance and thermal flux. At the BRT facility, 49.77% of the total produced flux was thermal, while only 26.40% and 23.84% of the total were contributed by resonance and fast flux. Resonance flux was the greatest contributor in the CRT facility, with 51.32% of total flux produced, while fast and thermal flux contributed 47.98% and 0.70%, respectively. Thus, FT is the most appropriate facility for fast flux. CRT can be utilized for both fast and resonance flux, while BRT is most suitable for thermal flux.

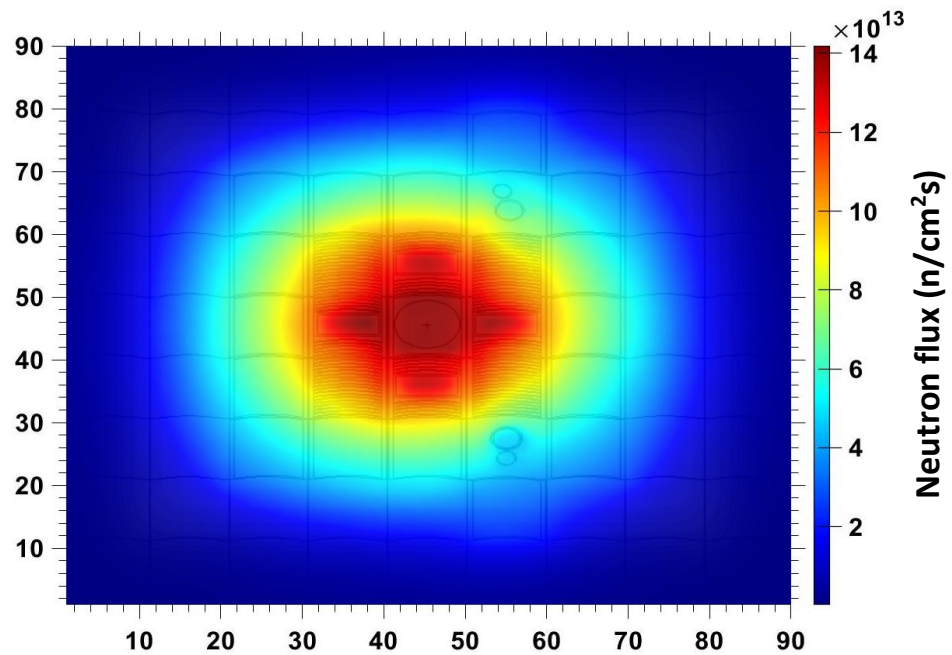


Figure 9. Neutron flux profile for the proposed MSTR-HPC core obtained by the MCNP simulation.

Table 4. Neutron Flux Spectrum In-Core Irradiation Facilities for MSTR-HPC.

	FT		BRT		CRT	
Thermal	4.57×10^{13}	32.21%	4.09×10^{13}	49.77%	2.92×10^{11}	0.70%
Resonance	4.58×10^{13}	32.28%	2.17×10^{13}	26.40%	2.13×10^{13}	51.32%
Fast	5.04×10^{13}	35.52%	1.96×10^{13}	23.84%	1.99×10^{13}	47.98%
Total	1.42×10^{14}	100.00%	8.23×10^{13}	100.00%	4.15×10^{13}	100.00%

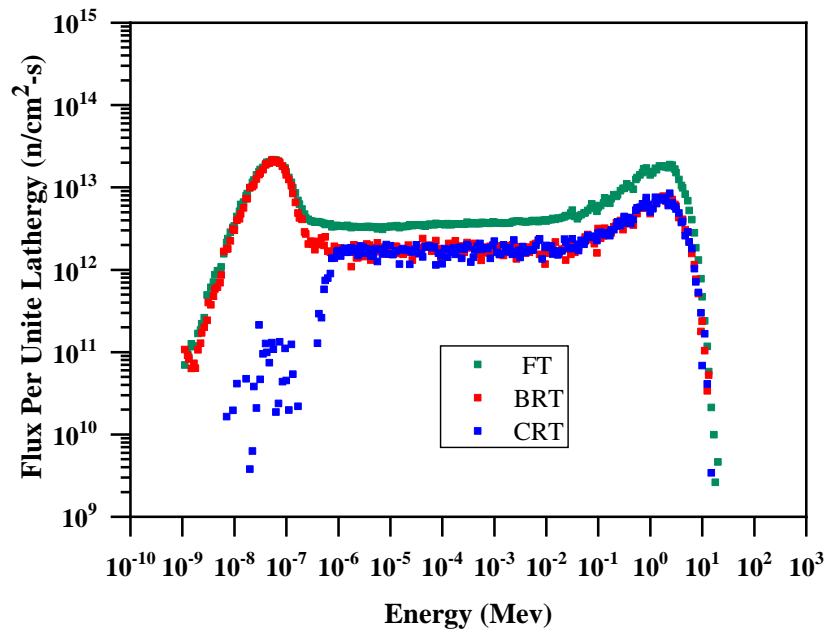


Figure 10. Neutron flux spectrum in-core irradiation facilities for the proposed MSTR-HPC.

The total neutron flux from in-core irradiation facilities is compared between current MSTR (Figure 1) and proposed MSTR-HPC (Figure 3) core configurations in Table 5. The MCNP simulation was carried out for both in the same way, but the power level was adjusted down to 200 kW for the current MSTR core configuration [10,13]. MSTR-

HPC achieves a maximum total neutron flux two orders of magnitude greater than the current MSTR core configuration, proving its effectiveness as a neutron flux enhancer. It is important to note that while the current MSTR core has 19 fuel-bearing elements [10,13], the proposed MSTR-HPC core has only eight fuel-bearing elements.

Table 5. Comparison of total neutron flux in-core irradiation facilities for the current MSTR and the MSTR-HPC core configurations.

	Current MSTR Core [10,13]				MSTR-HPC Core	
	HC	BRT	In-Core Irradiation Facilities		BRT	CRT
			CRT	FT		
Total Neutron Flux $\text{n cm}^2 \text{s}^{-1}$	$9.01 \times 10^{12} \pm$ 6.77×10^{11}	$5.26 \times 10^{12} \pm$ 4.79×10^{11}	$1.73 \times 10^{12} \pm$ 2.82×10^{11}	$1.42 \times 10^{14} \pm$ 1.78×10^{12}	$8.23 \times 10^{13} \pm$ 6.48×10^{12}	$4.22 \times 10^{13} \pm$ 4.77×10^{12}

5.4. Burnup Analysis

MSTR-HPC burnup analysis was carried out under the assumption that reflector block composite thicknesses were 1 cm for BeO and 6.6 cm for graphite. Tracking of fuel burnup at full power, or 2 MW, was performed by MCNP6. Figure 11 shows burnup time against k_{eff} for MSTR-HPC. Sixty-one days of continuous full-power operation were sustained by this reactor before subcriticality. The initial k_{eff} was calculated to be 1.03853 at time zero before dropping to 0.99964 (subcritical) on day 62. Twenty days of post-shutdown decay were included in the burnup simulation, with the calculated k_{eff} equal to 1.00035 after the first day of decaying, then increasing with time to 1.02291 after four decay days (or 66 totals, see Figure 11). After these first four days of decay, there was no significant change in k_{eff} . A 10-day cooling period is therefore assigned to the MSTR-HPC core, owing to the early k_{eff} plateau post-shutdown.

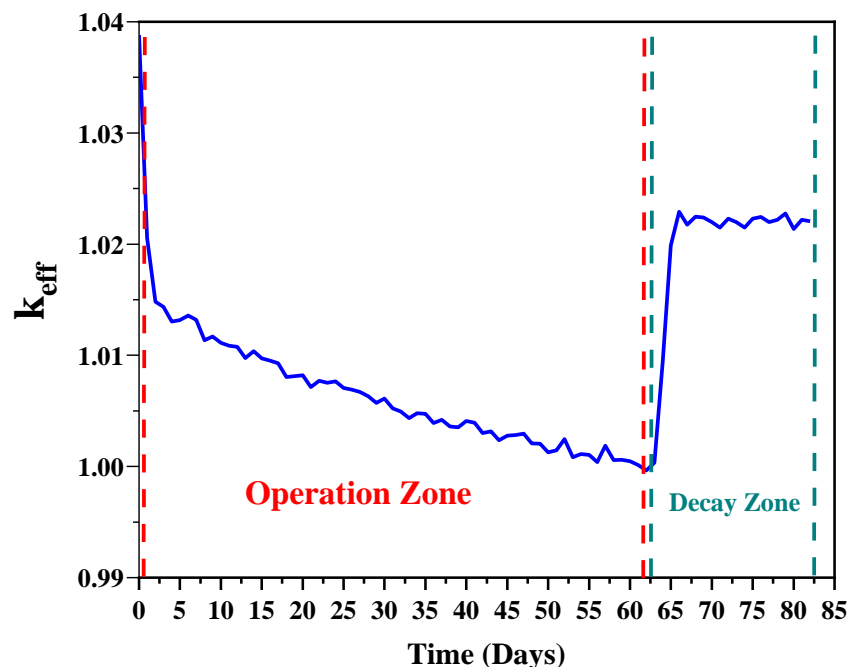


Figure 11. The burnup time versus the k_{eff} for the proposed MSTR-HPC.

Table 6 presents the post-burnup actinide inventory. Neither of the masses of U-235 or U-238 changed by a significant fraction. After 62 days of continuous operation, the mass of Pu-239 was found to be 14.1 g, increasing to 15.6 g after decaying for 10 days. This is caused by the short-lived isotope U-239 and Np-239 decaying to Pu-239. Total fissile material mass

was calculated at 0, 62, and 72 days and found to be 6153 g, 6011 g, and 6013 g, respectively. 9.01×10^{12} .

Table 6. MSTR-HPC's significant radionuclide inventories.

Isotopes	Mass (g)		
	0 Days	62 Days	72 Days
U-235	6.15×10^3	6.00×10^3	6.00×10^3
U-236	0.00	2.79×10^1	2.93×10^1
U-238	2.53×10^4	2.53×10^4	2.53×10^4
U-239	0.00	6.03×10^{-3}	-
Np-237	0.00	1.12×10^{-1}	1.36×10^{-1}
Np-239	0.00	8.54×10^{-1}	1.10×10^{-1}
Pu-238	0.00	6.23×10^{-4}	7.92×10^{-4}
Pu-239	0.00	1.41×10^1	1.56×10^1
Sr-90	0.00	2.84×10	2.97×10
Tc-99	0.00	3.13×10	3.49×10
Xe-135	0.00	2.26×10^{-2}	-
Cs-137	0.00	4.65×10	4.88×10
Sm-149	0.00	3.06×10^{-1}	3.52×10^{-1}

5.5. Determination of Hot-Channel

Both the clean core and burned core had their hot channel identified. There are 112 fuel plates in MSTR-HPC, illustrated in Figure 12, in sequence for each fuel element, numbers 1 to 18. Plates 6 through 13 were isolated and removed in order to allow for control rod insertion ("control rod channel"). These channels are filled with water. Figure 13 plots fuel plate energy deposition assuming a clean core. Fuel plate 14 (FP#14) in control rod 4 (CR4) was found to be the hottest fuel plate, located at the E4 position (see Figure 3). FP#14 is adjacent to the control rod channel, and the control rods are fully withdrawn.

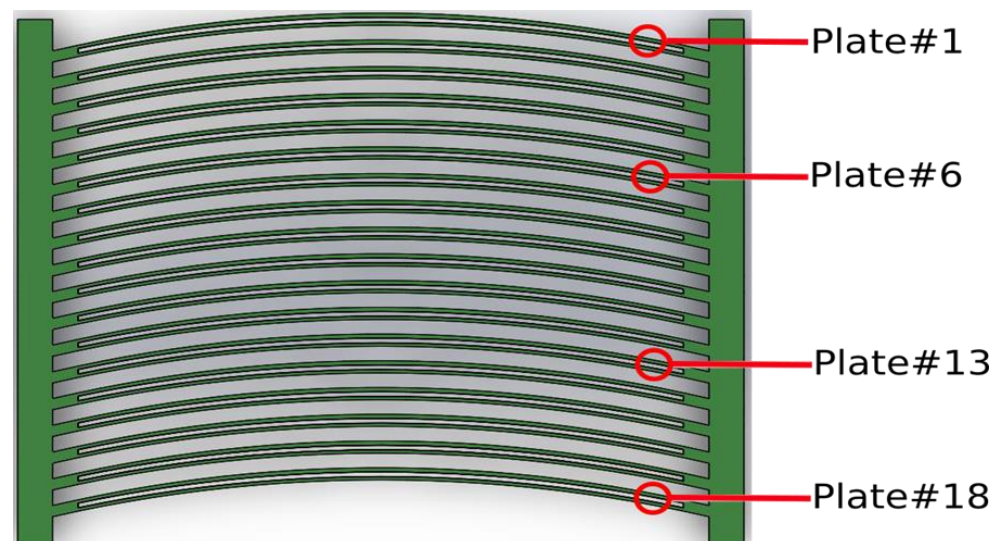


Figure 12. The order in which the fuel plates are arranged within each fuel element of MSTR-HPC.

The power output for FP#14 was calculated to be 32,416.06 W, the greatest power output among all fuel plates. 1.62% of the overall power distribution is produced by FP#14. The profile of the power distribution in FP#14 is variable along the fuel plate width, peaking sharply at the edges. This is caused by an increased water-to-fuel ratio locally in areas near the fuel meat edge. The hot channel was found to be located between FP#14 and FP#15 of CR4 for a clean core.

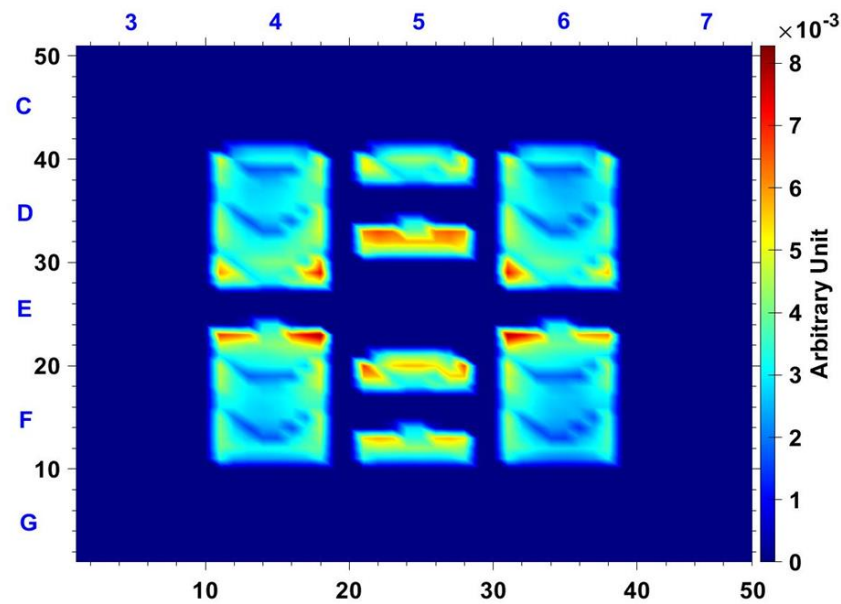


Figure 13. Energy deposition for MSTR-HPC clean core (C–G and 3–7 grid reference labels; blue colored).

Determining the burned core hot channel required implementing the burned materials into the MCNP model, then calculating energy deposition. The hot channel did not shift and was found to remain between FP#14 and FP#15 in the same location as it was in for the clean core. The hottest fuel plate also stayed the same: FP#14 of CR4. FP#14 had a power distribution of 32,330.84 W, contributing 1.61% of the total. Most fuel plates next to the control rod channel water saw significant non-uniform burnup relative to average fuel plates. With greater operation time, higher burnup in these specific plates will lead to reactivity issues in the core. A 90-degree rotation of the control rod fuel elements should therefore be considered in future research.

5.6. Thermal Hydraulic Behavior of MSTR-HPCs' Hot-Channel

In this work, the number of iterations taken into account in the CFD simulation was 232 CFD iterations. This number of iterations was found to be an adequate number of iterations for stabilizing the outlet temperature of the coolant channel. The determined average temperature for the coolant channel at the outlet of the model was 341.12 K. The calculated ΔT was 18.89 K, where ΔT is the temperature difference between the inlet and outlet. The temperature distribution profile along the height of the coolant channel is shown in Figure 14. The temperature at the inlet region was flat at the center 322.15 K, along with a little increase at the interfacing regions with convex and concave sides of the fuel plate. In the inlet region, no significant heating is generated, and the flow has not yet developed fully. In the middle of the coolant channel, the temperature at both interfacing regions reached a maximum of 383 K. However, at the center of the middle region of the coolant, the temperature reached 333 K. For both coolant interfaces (convex and concave sides of the fuel plate), the temperature distribution was similar due to the similarity of simulation conditions. At the outlet of the coolant channel, the temperature at both interfaces reached 359 K. For the center region, the flow exited the model at a temperature of 341 K, see Figure 14. The reason for lower temperatures at the interfacing regions for the coolant outlet is due to (1) the no-slip interface condition between the plate and the coolant and (2) the fuel, which is the heat source, does not extend to the inlet and the outlet edges of fuel plate. Hence, the coolant at the top of the interface receives no direct heat from the fuel meat. In addition, the top of the cladding in both fuel plates was set to be adiabatic for conservative analysis. It is worth noticing that in the monitored locations of the coolant channel, the temperature did not reach the boiling point of water at the considered pressure. The boiling point of water at 178.8 KPa is reported to be ~ 391 K [27].

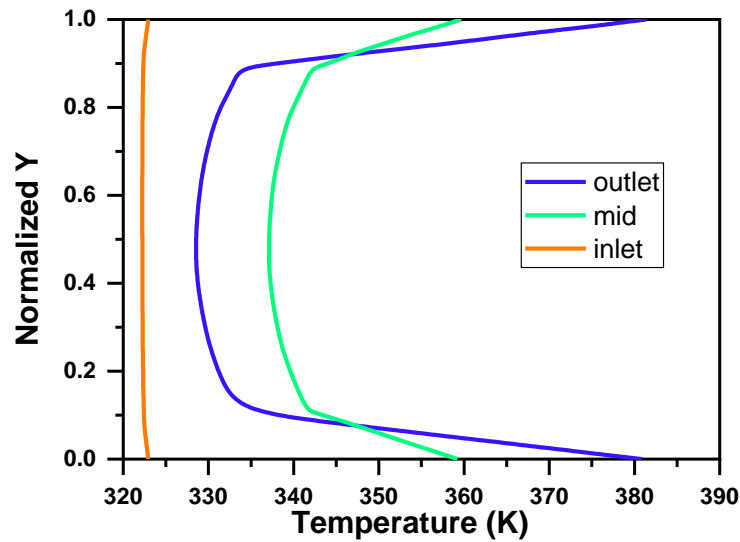


Figure 14. Temperature distribution along the inlet, mid, and outlet of the coolant channel.

The temperature contours for the convex sides of the fuel plate (containing fuel and clad) are shown in Figures 15 and 16, respectively. Temperature contours are used to analyze the heat flow in the fuel plate. They can be used to identify areas of high and low thermal conductivity, as well as areas where the fuel plate is being heated or cooled too quickly. The maximum temperature in the convex and concave sides of the fuel regions were 391.76 and 390.39 K, respectively. The maximum temperature attained in the convex and concave sides of aluminum-clad regions were 389.92 and 388.54 K, respectively. By considering the generated heat in the hottest fuel plate of the MSTR-HPC core, the determined temperature for fuel plate regions was below the safety limits. The safety limits to be considered from the safety point of view are the U-10Mo melting point (1150 °C = 1423.15 K), the delamination limits of U-10Mo plate-type fuel (~ 550 °C = 823.15 K), and the clad melting points (660 °C = 933.15 K) [28,29]. The velocity and pressure profiles are shown in Figures 17 and 18, respectively. At the coolant inlet, velocity started at 0.664 m/s and increased towards 0.8 m/s at the outlet of the coolant channel. The presented pressure profile is gauge pressure. The determined pressure difference (outlet to inlet) was 520 Pascal. At full operation power of the HPC core, the mass flow rate of 39.86 kg/s (10.644 gallon/s) was sufficient for removing the generated heat. An average pumping system in the current market can produce such a requirement. However, a pumping system with higher capacity can add extra safety assurance for removing the generated heat in the HPC core.

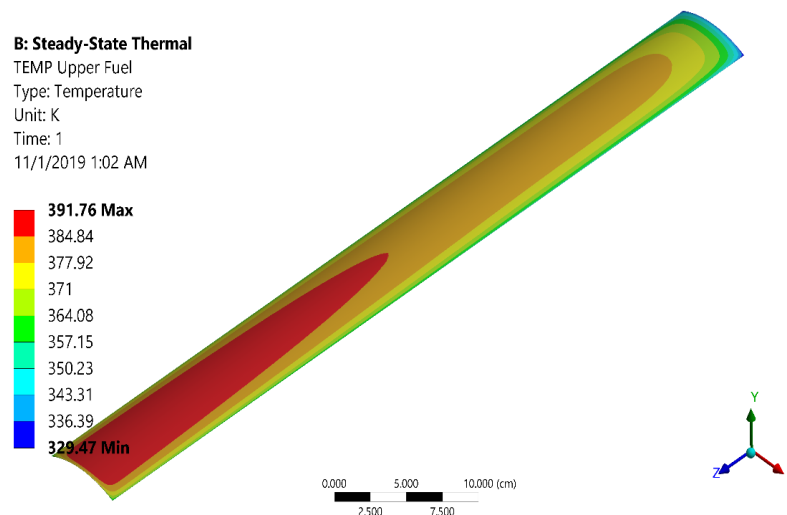


Figure 15. Temperature contours for the convex side of the fuel plate.

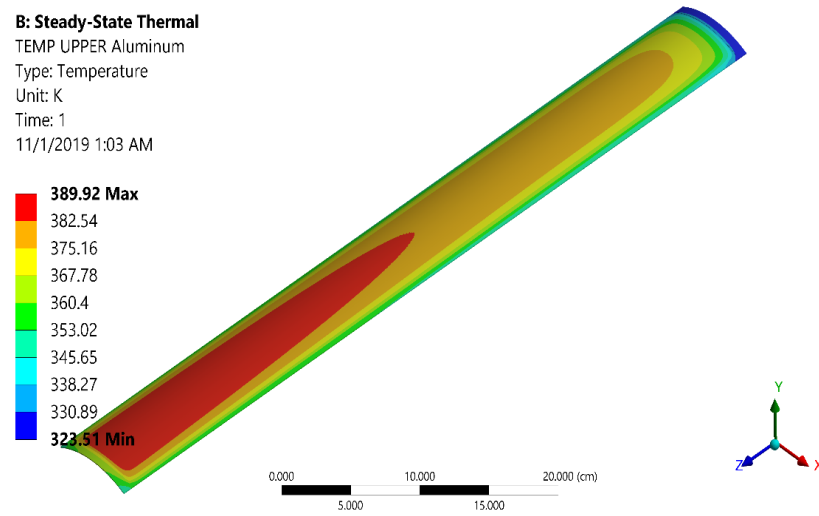


Figure 16. Temperature contours for the convex side of Clad.

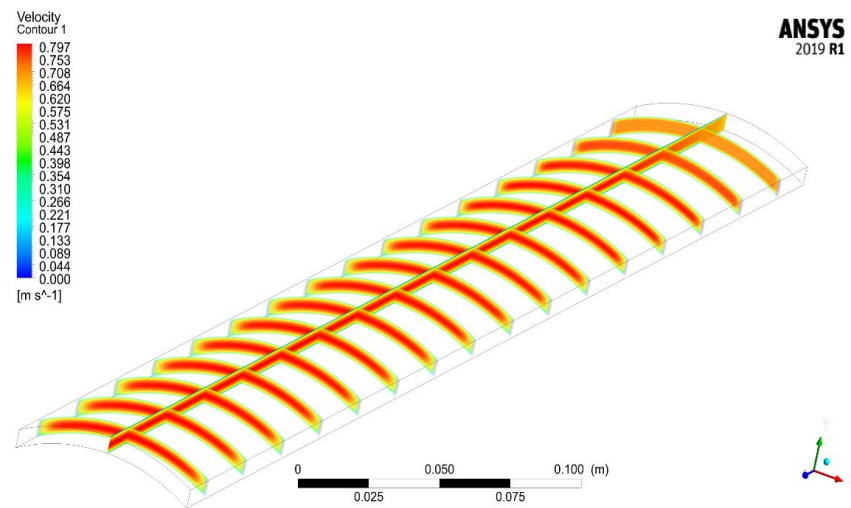


Figure 17. Velocity profile of coolant channel.

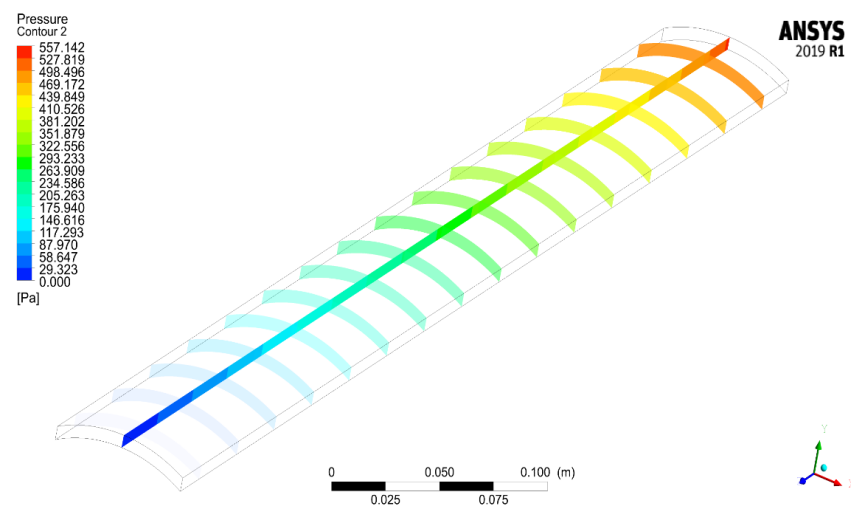


Figure 18. Pressure profile of coolant channel.

6. Conclusions

Adaptability and flexibility were introduced to the Missouri University of Science and Technology Reactor (MSTR) traditional design, allowing for greater support of a wide variety of advanced research and experimentation. Conceptual modifications of the MSTR features were crucial to this outcome. Such conceptual modifications were as follows: (1) the power level was updated; (2) the fuel meat type and design were both changed; (3) a flux trap facility was included; (4) the reactor core was reconfigured; and (5) the control rod boron concentration was increased to ensure an effective safety shutdown. The proposed MSTR-HPC core design was a compact core with four fuel elements, four partial fuel elements with control rod access, four control rods, three in-core irradiation facilities, and BeO/graphite composite reflector blocks surrounding the core. The reactivity coefficient (k_{eff}) of the modified MSTR-HPC was assessed with control rods completely withdrawn at room temperature, sustaining criticality with a k_{eff} of 1.03853, within the 4.5% $\Delta k/k$ constraint on excess reactivity. The BeO/graphite composite reflector blocks with 1 cm BeO thickness made this possible. The steel control rods had their boron concentration increased from 1.5% to 2% for effective safety shutdowns. Control rods 1 and 2 had to be paired for adequate shutdown margins to be achieved, while backup control rods provided additional safety measures in shutdown conditions.

The total MCNP-calculated neutron fluxes were $1.42 \times 10^{14} \pm 1.78 \times 10^{12}$, $8.23 \times 10^{13} \pm 6.48 \times 10^{12}$ and $4.15 \times 10^{13} \pm 4.63 \times 10^{12}$ $\text{n cm}^{-2} \text{s}^{-1}$ for FT, BRT, and CRT respectively. According to the energy spectra and flux magnitudes for certain irradiation locations, these were also the facilities most suitable for fast, resonance, and thermal fluxes. MSTR-HPC had a maximal flux two orders of magnitude greater than that obtainable from the current MSTR core configuration, demonstrating that significant potential flux enhancement is achievable. MSTR-HPC, with composite reflector blocks in place, is capable of sustaining 2 MW operations for up to two months. This allows longer experimental uptime and more research between refueling. The clean and burned core hot channel was situated between FP#14 and FP#15 of CR4, the backup control rod. Fuel elements with control rod channels produce larger proportional amounts of power. This means they have a faster depletion rate and require replacement more often.

Regarding the thermal-hydraulic evaluation for heat removal in the reactor core, a representational 3D model concerning the MSTR-HPC's two curved half-fuel plates with a single coolant channel in between was simulated using ANSYS Fluent. By applying maximum generated heat from "hot fuel plates" along with an assumption of high temperature, the simulated MSTR-HPC model did not exceed safety limits. At full operation power of MSTR-HPC, the mass flow rate of 39.86 kg/s (10.644 gallon/s) was sufficient for removing the generated heat. A typical pumping system that is available in the current market can be able to handle such a requirement. Pumps with higher capabilities, however, can add an extra layer of safety.

In conclusion, the conceptual design of the MSTR-HPC has demonstrated its flux enhancement capabilities while maintaining safety limits, which is of high importance in terms of enhancing reactor utilization for a larger window of time. Nevertheless, the proposed MSTR High-Power Configuration requires further thermal-hydraulic evaluations and should be the subject of future studies to demonstrate its safety and feasibility further. The high-power configuration should be further evaluated to ensure its performance and safety. Comprehensive thermal-hydraulic analysis should be conducted to evaluate the safety of the proposed configuration. Additionally, a sensitivity analysis should be conducted to identify any potential weaknesses in the proposed design.

Author Contributions: Conceptualization, A.B.A. and T.M.A. (Thaar M. Aljuwaya); methodology and software coding T.M.A. (Thaqal M. Alhuzaymi), M.M.A., T.M.A. (Thaar M. Aljuwaya) and A.B.A.; writing—original draft preparation, review, and editing T.M.A. (Thaqal M. Alhuzaymi), M.M.A., T.M.A. (Thaar M. Aljuwaya) and A.B.A.; supervision, A.B.A. All authors have read and agreed to the published version of the manuscript.

Funding: This research received no external funding.

Data Availability Statement: Not applicable.

Conflicts of Interest: The authors declare no conflict of interest.

References

- International Atomic Energy Agency. *Applications of Research Reactors*; International Atomic Energy Agency: Vienna, Austria, 2014.
- Barradas, N.P. Applications of research reactors. In *Encyclopedia of Nuclear Energy*; Greenspan, E., Ed.; Elsevier: Oxford, UK, 2021; pp. 8–25.
- Alnahdi, A.H.; Alghamdi, A.A.; Almarshad, A.I. Investigation of the Fuel Shape Impact on the MTR Reactor Parameters Using the Open MC Code. *Processes* **2023**, *11*, 637. [CrossRef]
- Son, H.M.; Song, K.; Kim, H.; Park, J. Conceptual design of narrow rectangular channel test section for research reactor application. *Nucl. Eng. Des.* **2023**, *403*, 112162. [CrossRef]
- International Atomic Energy Agency. *Utilization Related Design Features of Research Reactors: A Compendium*; International Atomic Energy Agency: Vienna, Austria, 2009.
- Marshall, J.L. *Fast Flux Test Facility (FFTF) Maintenance Provisions*; Hanford Engineering Development Lab.: Richland, WA, USA, 1981.
- Drell, S.; Hammer, D.; Cornwall, J.; Dyson, F.; Garwin, R. *Use of the Fast Flux Test Facility for Tritium Production*; Mitre Corp McLean VA Jason Program Office: McLean, VA, USA, 1996.
- Chandler, D.; Betzler, B.R.; Davidson, E.E.; Ilas, G. Modeling and simulation of a High Flux Isotope Reactor representative core model for updated performance and safety basis assessments. *Nucl. Eng. Des.* **2020**, *366*, 110752. [CrossRef]
- Morrell, D. *2012 Annual Report Research Reactor Infrastructure Program*; Idaho National Lab. (INL): Idaho Falls, ID, USA, 2012.
- Alqahtani, M.; Alajo, A.B. Characterization of prompt neutron spectrum of the Missouri University of Science and Technology Reactor. *Nucl. Eng. Des.* **2017**, *320*, 57–64. [CrossRef]
- Sipaun, S.; Usman, S. Prediction of Missouri S & T Reactor's natural convection with porous media approximation. *Nucl. Eng. Des.* **2015**, *285*, 241–248. [CrossRef]
- Stillman, J.; Feldman, E.; Foyto, L.; Kutikkad, K.; McKibben, J.; Peters, N.; Stevens, J. *Technical Basis in Support of the Conversion of the University of Missouri Research Reactor (MURR) Core from Highly-Enriched to Low-Enriched Uranium-Core Neutron Physics*; Argonne National Lab. (ANL): Argonne, IL, USA, 2012.
- Kulage, Z.A.; Castano, C.H.; Usman, S.; Mueller, G. Characterization of the neutron flux energy spectrum at the Missouri University of Science and Technology Research Reactor (MSTR). *Nucl. Eng. Des.* **2013**, *261*, 174–180. [CrossRef]
- Bonzer, W.; Carroll, C. *Safety Analysis Report for the Missouri University of Science and Technology Reactor—Revision 2*; University of Missouri: Rolla, MO, USA, 2008.
- O'Bryant, K.; Sipaun, S.; Usman, S.; Castano Giraldo, C.; Alajo, A. Determination of hot channel of Missouri S & T nuclear reactor. *Trans. Am. Nucl. Soc.* **2012**, *106*, 817–818.
- Wilson, E.; Jaluvka, D.; Hebden, A.; Stillman, J.; Jamison, L. *US High Performance Research Reactor Preliminary Design Milestone for Conversion to Low Enriched Uranium Fuel*; Argonne National Lab. (ANL): Argonne, IL, USA, 2019.
- Forrest, E.C. *Study of Turbulent Single-Phase Heat Transfer and Onset of Nucleate Boiling in High Aspect Ratio Mini-Channels to Support the MITR LEU Conversion*; Massachusetts Institute of Technology: Cambridge, MA, USA, 2014.
- Wilson, E.H.; Bergeron, A.; Stillman, J.A.; Heltemes, T.A.; Jaluvka, D.; Jamison, L. *U.S. High Performance Research Reactor Conversion Program: An Overview on Element Design*; Argonne National Laboratory: Lemont, IL, USA, 2017.
- Bergeron, A.; Wilson, E.; Yesilyurt, G.; Dunn, F.; Stevens, J.; Hu, L.-W.; Newson, T., Jr. *Low Enriched Uranium Core Design for the Massachusetts Institute of Technology Reactor (MITR) with Un-Finned 12 Mil-Thick Clad Umo Monolithic Fuel*; Argonne National Lab. (ANL): Argonne, IL, USA, 2013.
- Montierth, L.M. *Criticality Safety Evaluation for the Advanced Test Reactor Enhanced Low Enriched Uranium Fuel Elements*; Idaho National Lab. (INL): Idaho Falls, ID, USA, 2016.
- Meyer, M.K. *Investigation of the Cause of Low Blister Threshold Temperatures in the Rertr-12 and Afip-4 Experiments*; Idaho National Lab. (INL): Idaho Falls, ID, USA, 2012.
- Albarhoum, M. Reactivity cost for different top reflector materials in miniature neutron source reactors. *Prog. Nucl. Energy* **2012**, *58*, 39–44. [CrossRef]
- Dawahra, S.; Khattab, K.; Saba, G. Investigation of BeO as a reflector for the low power research reactor. *Prog. Nucl. Energy* **2015**, *81*, 1–5. [CrossRef]
- Werner, C.J. *MCNP Users Manual—Code Version 6.2.*; Los Alamos National Laboratory: Los Alamos, NM, USA, 2017.
- ANSYS. *Ansys Fluent in Ansys Workbench User's Guide*; ANSYS: Canonsburg, PA, USA, 2013.
- Material Management and Minimization (3M). Available online: <https://nnsa.energy.gov/aboutus/ourprograms/dnn/m3> (accessed on 26 September 2018).
- William, T.P. Water steam in thermal systems, subcommittee on properties of steam. In *ASME International Steam Tables for Industrial Use: Based on the IAPWS Industrial Formulation 1997 for the Thermodynamic Properties of Water and Steam (IAPWS-IF97)*; American Society of Mechanical Engineers: New York, NY, USA, 2000.

28. Daxin, G.; Huang, S.; Wang, G.; Wang, K. Heat Transfer Calculation on Plate-Type Fuel Assembly of High Flux Research Reactor. *Sci. Technol. Nucl. Install.* **2015**, *2015*, 1–13. [[CrossRef](#)]
29. Robinson, A.; Chang, G.; Keiser, D., Jr.; Wachs, D.; Porter, D. *Irradiation Performance of u-mo Alloy Based 'Monolithic' Plate-Type Fuel-Design Selection*; Idaho National Lab. (INL): Idaho Falls, ID, USA, 2009.

Disclaimer/Publisher's Note: The statements, opinions and data contained in all publications are solely those of the individual author(s) and contributor(s) and not of MDPI and/or the editor(s). MDPI and/or the editor(s) disclaim responsibility for any injury to people or property resulting from any ideas, methods, instructions or products referred to in the content.